International Journal of Civil Engineering (2019) 17:723–735
https://doi.org/10.1007/s40999-018-0348-2

RESEARCH PAPER

Assessment of Ground Improvement by Vibro-compaction Method for Liquefiable Deposits from In-Situ Testing Data

Wei Duan[1] · Guojun Cai[1] · Songyu Liu[1] · Jun Yuan[1] · Anand J. Puppala[2]

Received: 1 February 2018 / Revised: 2 June 2018 / Accepted: 19 July 2018 / Published online: 9 August 2018

Abstract
Seismic piezocone penetration tests, resistivity piezocone penetration tests, and standard penetration tests (SPT) were conducted to quantitatively assess the effects of soil improvement by vibro-compaction. The differences of piezocone penetration test (CPTU) basis readings, improvement index for densification, electrical resistivity of soils, and state parameters before and after ground treatment were analyzed, and the effect of the increase in stiffness on the site response was also analyzed for the effect of densification. A combination of shear wave velocity, V_s, and cone tip resistance, q_c, was used for the interpretation of the changes of coefficient of earth pressure at rest, K_0, and mean grain size, D_{50}, before and after compaction. The dissipation process of excess pore pressures during vibro-compaction has been presented to show the effect of drainage. In addition, liquefaction potential was also estimated by CPTU and SPT for its effect of reinforcement. The results showed that the liquefied soil was densified and the use of a combination of in-situ tests could be used for ground improvement needed to mitigate liquefaction.

Keywords Vibro-compaction · SCPTU · RCPTU · Ground improvement · Liquefiable deposits

1 Introduction

Vibro-compaction, as a method of deep ground improvement, has been widely used to densify cohesionless and cohesive soils and to reduce the potential for earthquake-induced liquefaction [1–3]. The evaluation and quality control of vibro-compaction ground improvement for liquefaction mitigation is a major and important task for the state of practice [4–6]. In general, in situ tests, along with laboratory tests, are applied to assess the effect of ground improvement. However, the accuracy of laboratory tests is highly dependent on sample disturbance, and obtaining high-quality, undisturbed samples of cohesionless soil are difficult and costly for any routine project [7]. Thus, in situ tests have been, and still are, the dominant method in engineering practice for evaluating ground improvement.

Among the in-situ tests, the cone penetration test (CPT) is often used for assessing ground improvement and checking the degree of improvement that has been achieved [5]. The modern advanced piezocone penetration test (CPTU), as an extension of the CPT, has been preferred as one of the most useful tools to assess the quality of ground improvement [2, 8]. The CPTU provides continuous profiling of soil behavior type and CPTU parameters, cone tip resistance (q_t), sleeve frictional resistance (f_s), and pore water pressure (u), simultaneously. Recently, the field index of shear wave velocity (V_s) measurements, directly correlating to the density and stiffness of soils, became prevalent [9]. Furthermore, the V_s is closely related to the cyclic resistance ratio (CRR) in the simplified shear stress procedure of liquefaction potential assessment [10]. Thus, the seismic piezocone penetration tests (SCPTU) attract more attention

✉ Guojun Cai
focuscai@163.com; 101011362@seu.edu.cn

Wei Duan
zbdxdw@163.com; 230169537@seu.edu.cn

Songyu Liu
liusy@seu.edu.cn

Jun Yuan
15950595709@163.com; 220163549@seu.edu.cn

Anand J. Puppala
anand@uta.edu

[1] Institute of Geotechnical Engineering, Southeast University, Si Pai Lou No. 2, Nanjing 210096, Jiangsu, China

[2] Department of Civil Engineering, The University of Texas at Arlington, 701 South Nedderman Drive, Arlington, TX 76019, USA

to monitor and document the effect of ground improvement [11]. In addition, resistivity is a function of soil density, and thus, the resistivity piezocone penetration tests (RCPTU) have the potential benefit of providing additional, independent information about increases in soil density resulting from ground improvement efforts [12]. However, limited research has been done using combinations of in-situ tests such as SCPTU and RCPTU to assess ground improvement efforts. It is commonly understood that liquefiable ground improvement mechanisms (e.g., densification, drainage, and/or reinforcement) also provide the basis for applying effective mitigation efforts. Therefore, it is necessary to perform this work.

This paper describes the results of SCPTU tests, RCPTU tests, pore water pressure measurement, and SPT tests carried out in potentially liquefiable silts and sands improved by vibro-compaction (vibratory probe). The results indicate that field penetration testing for the quality control of ground improvement is feasible and verifies the potential benefits of the use of a combination of in situ tests.

2 Vibro-compaction Technology

Cohesionless soils are most effectively densified by vibratory means. In general, the equipment consists of three parts: a 7 ton vibrator with powerpack, a cross-shaped vibro-wing, and a 50-ton crawler crane (see Fig. 1a). It should be noted that several different types of compaction probes, such as the Terra probe, Y-probe, and vibro-rod, have been developed and applied [13]. A new crisscross section vibratory probe, 0.6 m wide and 15 m in length, has been developed and used as a resonance compaction probe in this study. The cross-shaped vibration wing is a cylindrical probe containing two perpendicular steel plates, as shown in Fig. 1b. The probe also has circular openings 0.1 m in diameter and 0.8 m apart, which act to reduce probe impedance, provide better contact with soil, and increase the drainage of excess pore water pressure caused by compaction construction. The most important aspect of the probe design is the semicircular bulge teeth along the side and the zigzag bulge teeth in the end, which can reduce the soil resistance during the probe penetration process. Meanwhile, the vibration energy will transmit to a larger area and further improve the compaction effect. Since the cross-sectional area has been reduced, the lighter weight can give a relatively larger amplitude of displacement for densification soil. The vertical oscillation is generated by eccentric weights situated at the top of the cylinder. Vibration frequency can be altered, varying from 0 to 20 Hz, during ground improvement for obtaining the resonance frequency. In practice, resonance frequency depends on the subsurface soil type and the underground water table. A centrifugal force of 360 kN is generated during the penetration process, which causes a maximum movement of the tip of about 2 cm. The vibro-wing is lowered to the necessary treatment depth at a rate of 2.0 m/min and raised at a rate of 1.2 m/min.

With an increase in the proportion and plasticity of fines in the soil, the effectiveness of the vibratory compaction will decrease. As the fines' content increases, the permeability of the soil being treated will reduce [14]. This restricts drainage and causes difficulties in the denser packing of soil

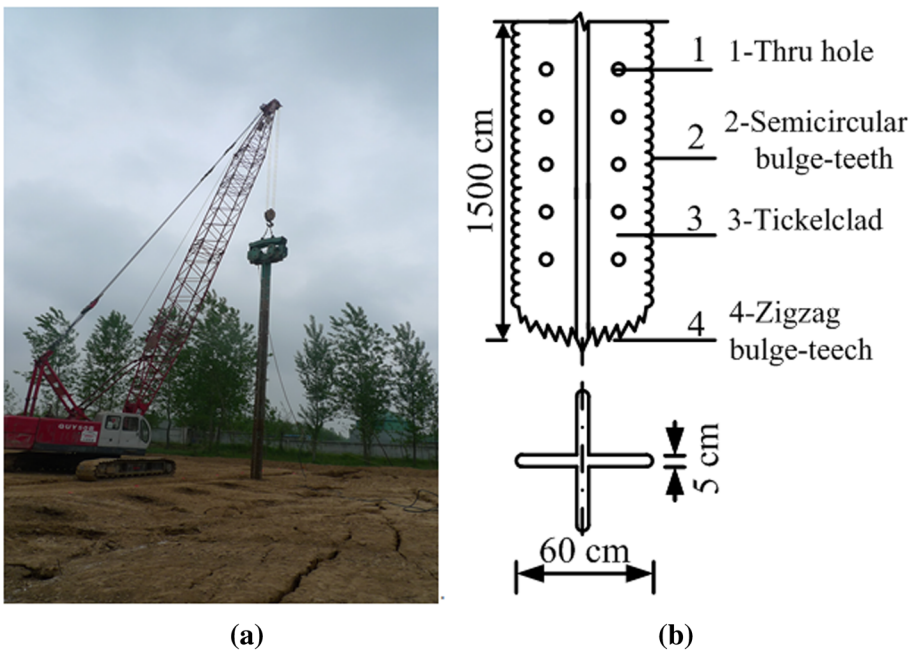

Fig. 1 Cross-shaped vibration equipment: **a** base machine in the field and **b** crisscross section vibratory probe

particles. The transmission of vibration to the surrounding soil is attenuated when high pore pressures are generated or liquefaction occurs in the soil adjacent to the soil being vibrated. Thus, the main range of influence of the process is greatly reduced and ground treatment procedures should be adjusted and time allowed for the dissipation of excess pore pressures before further treatment is applied.

Distinguishing between layers of loose sands and soils with high silt contents during site exploration is difficult. The presence of increased fines content affects the evaluation of the degree of ground treatment achieved. It should be noted that tip resistance is a relatively insensitive measure of improvement in strength and stiffness in silts and clays. The change of pore pressure response from positive to strongly negative, during the process of penetration, indicates improvement in the liquefaction resistance of silts [15].

Often, the aim of potentially liquefiable ground improvement is for one or more of the following:

- densification effect (that is, increase strength and stiffness);
- drainage effect (that is, the dissipation process of excess pore pressures);
- reinforcement effect (that is, decreased liquefaction potential).

3 Field Piezocone Penetration Testing

The CPT, or CPTU, has always been used as an in-situ testing method for determining the geotechnical engineering properties of the ground and delineating soil stratigraphy [16]. For CPTU testing, pressure can be measured at one of two locations, either on the face (u_1) of the cone tip or behind the cone tip (u_2). Due to developments in the in-situ test technique, data acquisition, and processing software, during the last few decades, the SCPTU and RCPTU testing can provide not only base readings of piezocone, but also electrical resistivity (ρ) and V_s, respectively. A schematic of the SCPTU and RCPTU probes can be found in the literature [11, 17].

The SCPTU and RCPTU tests were conducted using a lightweight truck with a 20 ton capacity hydraulic system, in accordance with ASTM D 5778 [18] and Lunne et al. [19]. All CPTU tests were performed at the standard penetration rate of 20 mm/s and nearly continuous readings were collected at approximately 5 cm intervals. It should be noted that seismic V_s measurements were made at 1.0 m intervals. The ρ was measured using four additional copper electrode array resistivity modules with an internal circuit system behind the probe.

The section area of the cylindrical cone penetrometer was 10 cm^2 and had a tip angle of 60°. The surface area of the friction cylinder was 150 cm^2 and had a pore pressure filter element located just behind the shoulder in the u_2 position. The ground water table at the test site varied from 3.8 to 6.0 m, and was recorded immediately after the CPTU tests. A correction for total cone tip resistance should be applied to account for the inner geometry design of the cone for obtaining the actual total stress (q_t). The following relationship was used in the correction of q_c [20]:

$$q_t = q_c + (1 - a) \times u_2, \tag{1}$$

where q_t is the total cone resistance corrected for unequal end-area ratio and pore pressure effects, q_c is the measured total cone resistance, a is the area ratio of the cone, and u_2 is the pore pressure acting behind the cone.

3.1 Site Description

The test site was situated in an area of high construction activity on a highway in Suqian, Jiangsu Province, China. The schematic of in-situ testing and construction of vibro-compaction is shown in Fig. 2. A set of CPTU soundings were conducted to assess the compaction performance of ground improvement of the liquefaction-susceptible layer before and after vibro-compaction (Fig. 3). It is necessary that CPTU soundings should be conducted near one another before, during, and after ground improvement. According to the local design experience, the mean values of a_{max} and M_w were measured as 0.15 g and 8, respectively. The mean penetration depth of the CPTU tests was 20 m. The mean value of the

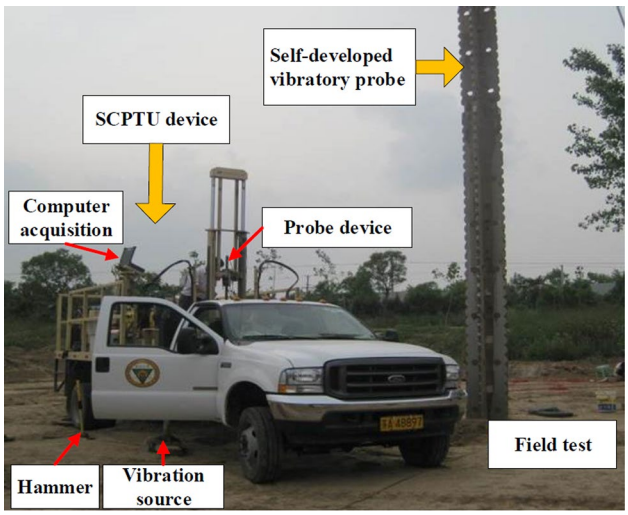

Fig. 2 Schematic of field test and vibro-compaction

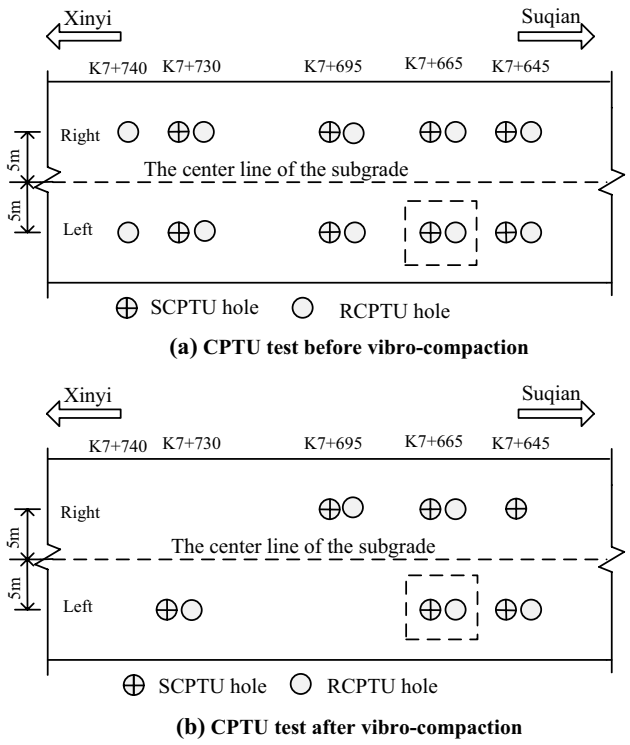

Fig. 3 Layout of CPTU soundings at the Suqian-Xinyi highway site

underground water table at the test site was about 4.0 m. The soil stratum consisted of fill, loose silty clay, loose silty sand, and sand. The liquefaction-susceptible layer was the silty sand ranging from 5.0 to 15.0 m, and was, therefore, considered in this study.

4 Evaluation of the Effect of Densification

4.1 Relative Increase Index

Increases in penetration resistance are the result of decreases in void ratio or increases in stress. Thus, the quality control of densification is often based on the increment of penetration resistance. It is difficult to reflect the degree of increment by penetration resistance. The relative increase index (I_d) is a quantitative measure of the degree of ground improvement by densification [21]. Its form is the same as the relative error and could be used for the establishment of expected improvement ranges, which are independent of the correlations for the given soil classifications and the initial soil states. The I_d can be used for evaluating the changes of resistance and the degree of densification. The improvement index is given by the following formula:

$$I_d = \frac{q_{t,after} - q_{t,before}}{q_{t,before}} = \frac{q_{t,after}}{q_{t,before}} - 1, \quad (2)$$

where $q_{t,before}$ and $q_{t,after}$ are the CPTU correlated tip resistances at the same CPTU points before and after densification, respectively.

Figure 4 presents the CPTU profiles and incremental improvement index before and after vibro-compaction. It should be noted that increases in q_t and f_s indicate that the strength of silty sand has been increased by the effectiveness of resonance. The increase in horizontal effective stress can be used prior to the compaction ratio of f_s [22]. As shown in Fig. 4, an average increase of f_s is approximately 2, suggesting that the horizontal stress has been increased due to

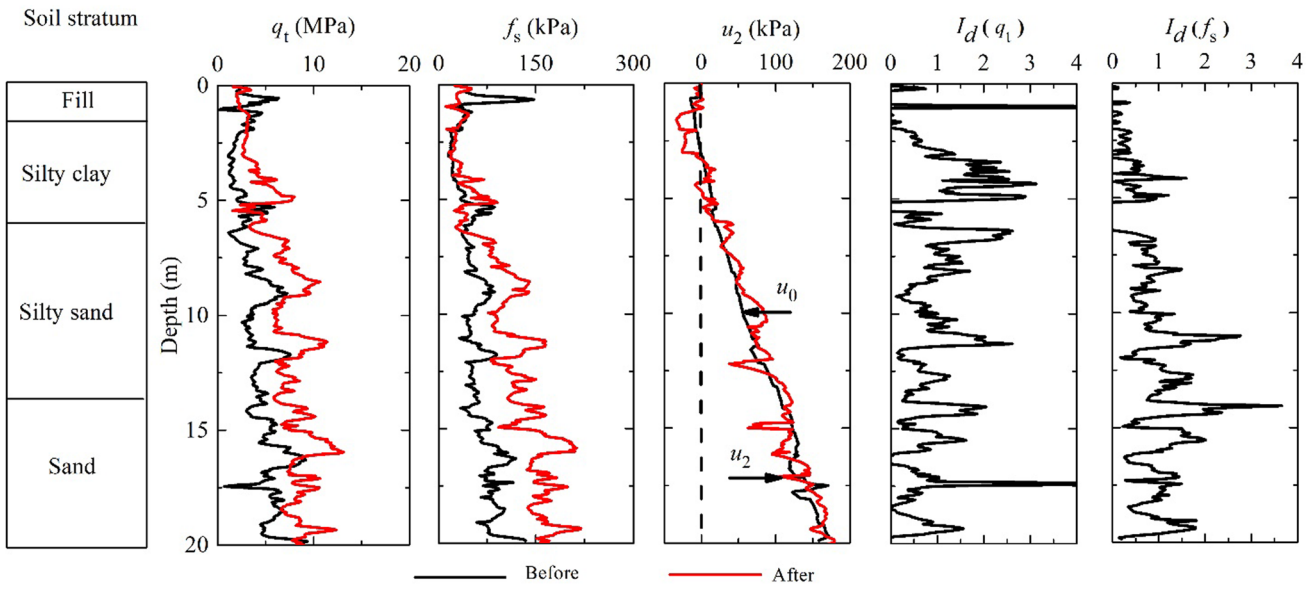

Fig. 4 CPTU profiles and incremental improvement index before and after vibro-compaction

compaction. The variation of u_2 with depths illustrates that some rapid variation in the dilation characteristics of the soil (layered effect) before vibro-compaction exists. Following treatment, the response is more consistently positive due to the mixing of soil layers by compaction. The range of I_d values varies from 0.5 to 3, corresponding to the depths between 3 and 5, and 11and 14 m, respectively. A maximum relative increase index of 4.0 was estimated for the sand layer at a depth of 17.5 m. The results showed that the I_d parameter gives a more intuitive sense for compaction and can be used as a quantitative index for estimating the effectiveness of the vibro-compaction ground improvement.

4.2 State Parameter

The state parameter (Ψ) is defined as a measure of the deviation between the current void ratio (e) and the critical void ratio (e_c) at the same stress level, as shown in Fig. 5. The parameter Ψ introduced by Been and Jefferies [23] can combine the effect of the void ratio and stress level by itself. The parameter Ψ is also an index to measure sand's dilatancy during shearing. A negative Ψ indicates dense, dilative soils, whereas a positive Ψ indicates loose, contractive soils [24].

Been et al. [25] developed an approach to derive Ψ from a CPT, and studied an extension that includes undrained and partially drained conditions using the normalized parameter B_q [26]:

$$\psi = -\frac{\ln[Q_P 1 - B_q/\bar{k}]}{\bar{m}}, \tag{3}$$

where Q_P is a form of normalized cone resistance based on mean stresses, and $\bar{k}$ and $\bar{m}$ continue primarily as functions of compressibility. The specific solution process can be found in the literature [25, 26].

The negative value or positive value of a state parameter is directly used for identification of the behavior of dilative or contractive in the initial screening of low-risk projects. In fact, Jefferies and Been [27] suggested that coarse-grained, ideal soils, with a state parameter less than -0.05 ($\psi < -0.05$), will be dilative at large strains. Figure 6 presents the changes of ψ along depths before and after vibro-compaction. Consequently, according to the standard, the mean value of the ψ values of the depths for most soils before vibro-compaction are more than -0.05. It should be noted from Fig. 6 that most ψ values are less than -0.05 after vibro-compaction and the profile of the state parameter is further away from the zero axis than that before vibro-compaction. This comparison illustrates that, as void ratio decreases, the soils become denser due to the effect of vibro-compaction.

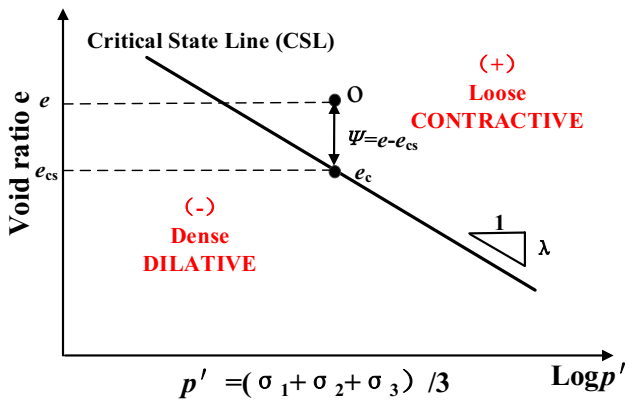

Fig. 5 Definition of state parameter

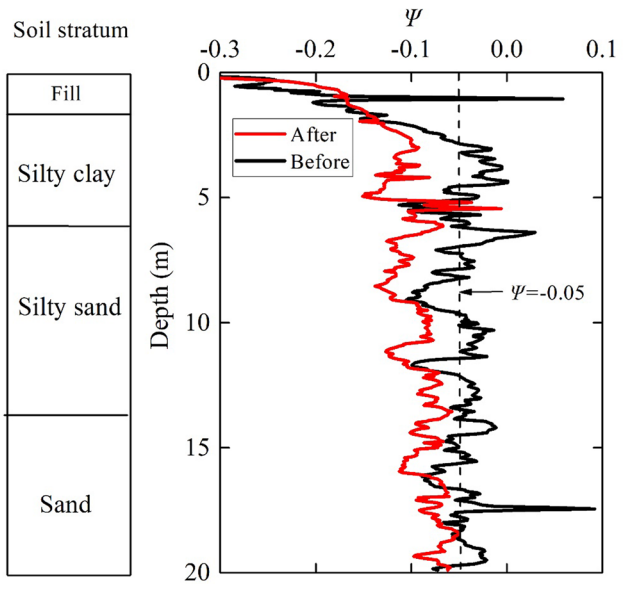

Fig. 6 Change of state parameter along depth before and after vibro-compaction

4.3 Electrical Resistivity

Resistivity measurements can be treated as a further indicator of soil improvement and used for the evaluation of densification [12]. The RCPTU can provide base piezocone readings and electrical resistivity of the soil. The method for interpretation of resistivity involves using Archie's Law, which can relate the resistivity of the pore fluid and porosity (soil density) to the bulk soil resistivity. This method is suitable for saturated cohesionless soil and pure sand, and the equation is written in the form of the following:

$$\rho_b = \rho_f \cdot a \cdot n^{-m}, \tag{4}$$

where ρ_b = buck soil resistivity (Ω m); ρ_f = buck soil resistivity (Ω m); n = soil porosity (void volume/total volume);

a,m = soil constants related, respectively, to the coefficient of saturation and the cementation factor.

It is assumed that the soil constants remain constant during the process of densification. Taking before and after ground improvement into consideration, the Eq. (4) can be written using the following forms [12]:

$$\rho'_b/\rho_b = (\rho'_f/\rho_f) \cdot (n'/n)^{-m}, \tag{5a}$$

or

$$n'/n = ((\rho'_b/\rho_b) \cdot (\rho_f/\rho'_f))^{-1/m}, \tag{5b}$$

where (′) represents post-densification values; and the m varies from 1.3 to 2.2 for granular soils with non-conductive grains. It should be noted that the void ratio (e) can be calculated by the n value ($e = n/(1 - n)$). Equation (5b) can be used for assessing the ratio of before and after densification porosity with RCPTU measurements when the value of m is given.

Figure 7 depicts the representative electrical resistivity profiles pre- and post-vibro-compaction ground treatment from the study site, including the calculated porosity ratio (assuming m values of 1.3 and 2.2). It has been shown in the literature that groundwater resistivity does not change during the densification process [28, 29]. It can be observed that post-densification resistivity is higher than pre-densification. Once the pre- and post-densification resistivities are known, the porosity ratio can be calculated by Eq. (5b). Two porosity ratio profiles are depicted to show the effects of changing the (m) value and suggest that the porosity was reduced. A comparison of results indicates that the porosity ratio of the silt sand is less than 1.0 for both m values of 1.3 and 2.2, for the densification process of ground improvement.

In practice, when the probe penetrates the ground, the zone of soil is disturbed with the magnitude and distribution of volumetric strain varying with density and stress level. Density and stress level are both increased during vibro-compaction ground improvement.

4.4 Small Strain Shear Modulus

The V_s can be treated as an effective stress parameter that is closely related to the soil maximum shear modulus or small strain stiffness ($G_{max} = \rho_T V_s^2$) [30]. As V_s directly relates to shear modulus, it can be considered an important parameter in earthquake analysis. In addition, G_{max} can be related to the site deformation potential during a seismic action. The accuracy of the V_s values measured in the laboratory tests is very sensitive to sample disturbance. Thus, in situ testing has become the most reliable method to obtain the V_s of varying depths and can be measured by SCPTU. A statistical relationship has been proposed by Mayne et al. [31] linking the total mass density data from all types of soil, to V_s, in m/s and depth, z, in m ($n = 727$; $r^2 = 0.730$):

$$\rho_T \approx 1 + \frac{1}{0.614 + 58.7(\log z + 1.095)/V_s}, \tag{6}$$

where $\rho_T = \gamma_T/g$ = mass density of soil (g/cm^3).

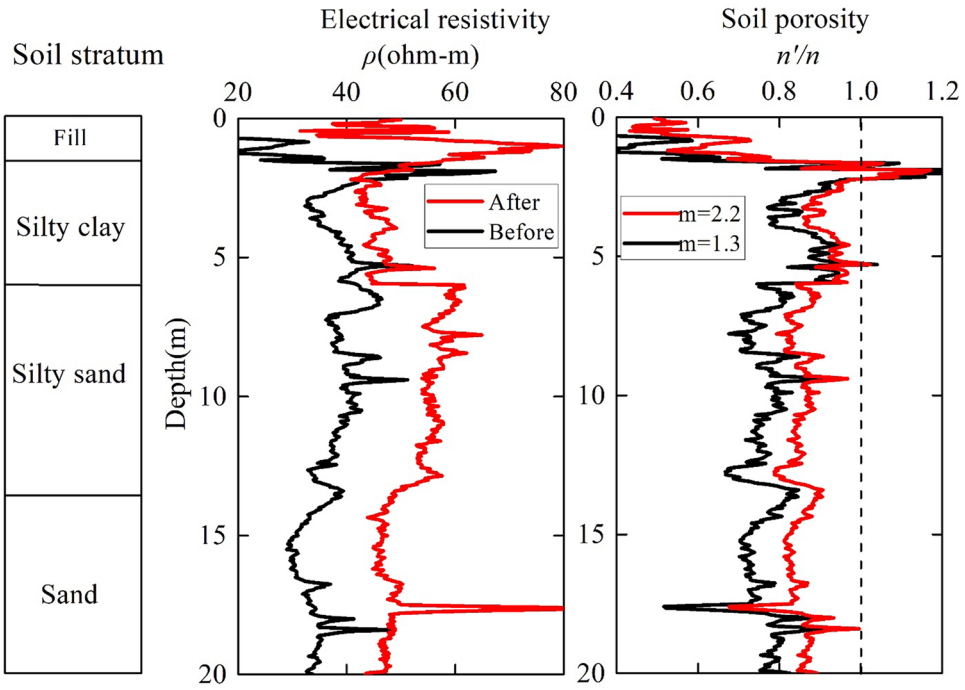

Fig. 7 Pre-and post-densification resistivity data and calculated porosity ratio in study site

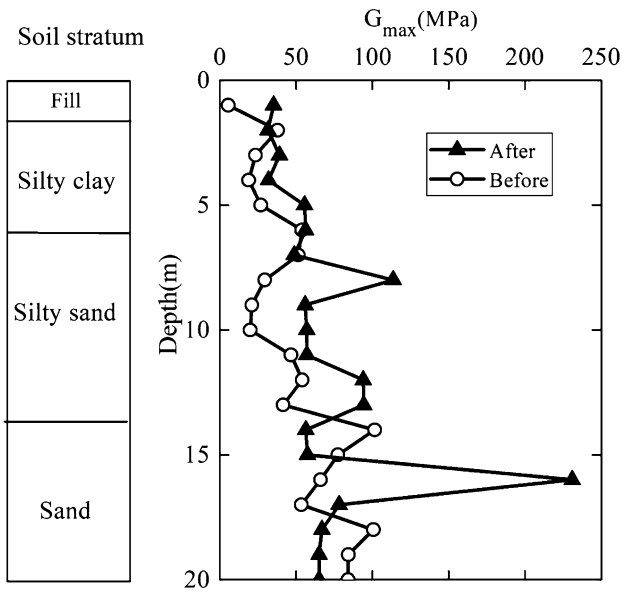

Fig. 8 Small strain stiffness profiles before and after improvement

Figure 8 displays the G_{max} profiles before and after ground improvement. There is a clear increase in small strain stiffness following ground improvement. The results show that an increase of deformation resistance at various depths occurs after a significant soil improvement by vibro-compaction, which is an effect that could have great practical significance.

4.5 Using a Combination of V_s and q_c

It is well known that both V_s and q_c are affected by vertical stress, horizontal stress and density [32]. It is necessary to attempt to use a combination of V_s and q_c to derive some soil properties. The G_o/q_c ratio can be used to interpret SCPTU data. The G_o/q_c ratio is very useful for connecting elastic stiffness to ultimate strength. Baldi et al. [33] studied that G_o/q_c ratio decreases with increasing relative density (D_r) for q_c increasing much faster than G_o with D_r. A statistical correlation combined expression for q_c and G_o to evaluate the coefficient of earth pressure at rest, K_0, was suggested by Eslaamizaad and Robertson [34]. The coefficient of earth pressure at rest (K_o) is defined as the ratio of horizontal effective stress to the vertical effective stress. This expression can eliminate the effect of D_r:

$$G_0/p_a = 334.90(q_t/p_a)^{0.25}(\sigma'_v/p_a)^{0.332}K_0^{0.462}, \quad (7a)$$

or

$$K_0 = 3.4 \times 10^{(-6)}(p_a/\sigma'_v)^{0.718}\left[(G_0/p_a)/(q_t/p_a)^{0.25}\right]^{2.165}, \quad (7b)$$

where p_a is the atmospheric pressure (100 kPa). The change of K_0 caused by ground improvement can be assessed by Eq. (7b) when the assumption of σ'_v is that there is no change in any depth during the densification.

If K_0 increases, the combined parameter $\left[(G_0/P_a)/(q'_t/P_a)^{0.25}\right]$ will be increased for a known depth or σ'_v. A clear increasing trend as a result of vibro-compaction can be seen in Fig. 9.

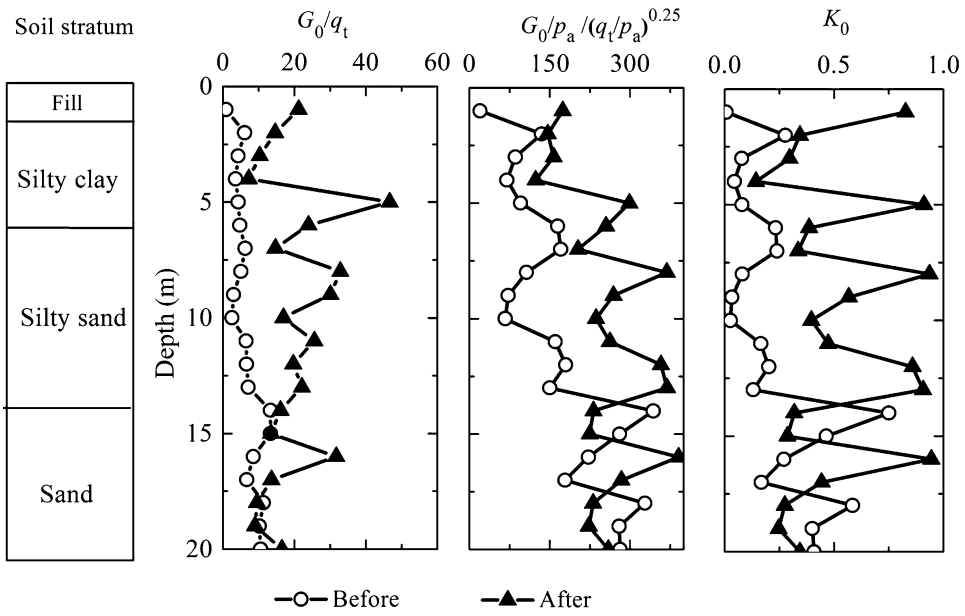

Fig. 9 K_0 profiles from the combination of V_s and q_c before and after vibro-compaction

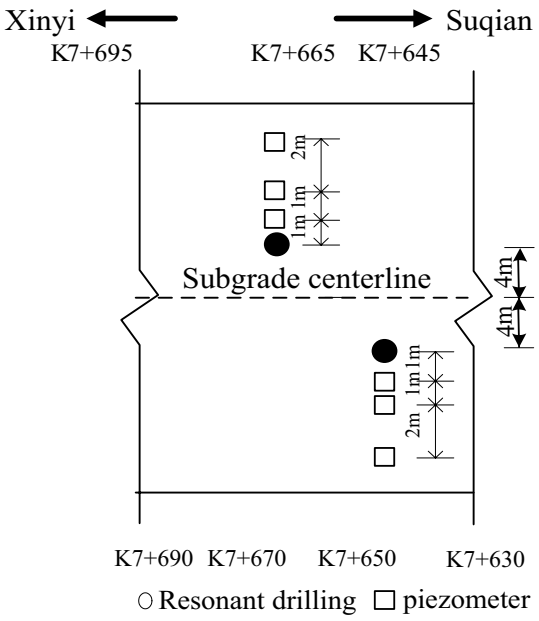

Fig. 10 Layout of pore pressure gauge

5 Evaluation of the Effect of Densification

The vibration pore water pressure in saturated soil will be caused by the vertically oscillating probe. The increasing pore water pressure may result in soil liquefaction. Once high pore pressures are generated, or liquefaction occurs in the soil adjacent to the soil being vibrated, the transmission of vibration is limited and the scope of reinforcement is affected. Therefore, the study of variation laws related to pore water pressure during and after vibro-compaction is very important for construction engineering. Figure 10 presents layouts of resonant drilling and piezometer. A total of 15 piezometers were conducted at the test site, with each layer having three piezometers and the distance from the resonant drilling are 1, 2, and 4 m, respectively.

Figure 11 presents the dissipation process of excess pore pressure at the same depth for different distances from a single resonant hole (K7+645). As shown in Fig. 12, the actual used time is about 28 min. The excess pore water pressure appears to reach a peak value several times, and this is due to the action of the vertically oscillating probe. The excess pore water pressure, measured by three piezometers in the same layer, reached the peak values at the same time. At each depth, the peak values of the excess pore pressure decrease with the increasing distance from the resonant drilling. The excess pore pressure is small at a distance of 4 m from the resonant drilling. Thus, the maximum influential range of resonance construction is greater than 4 m.

Figure 12 presents the dissipation process of excess pore pressure at 1 and 2 m from the vibration point. It

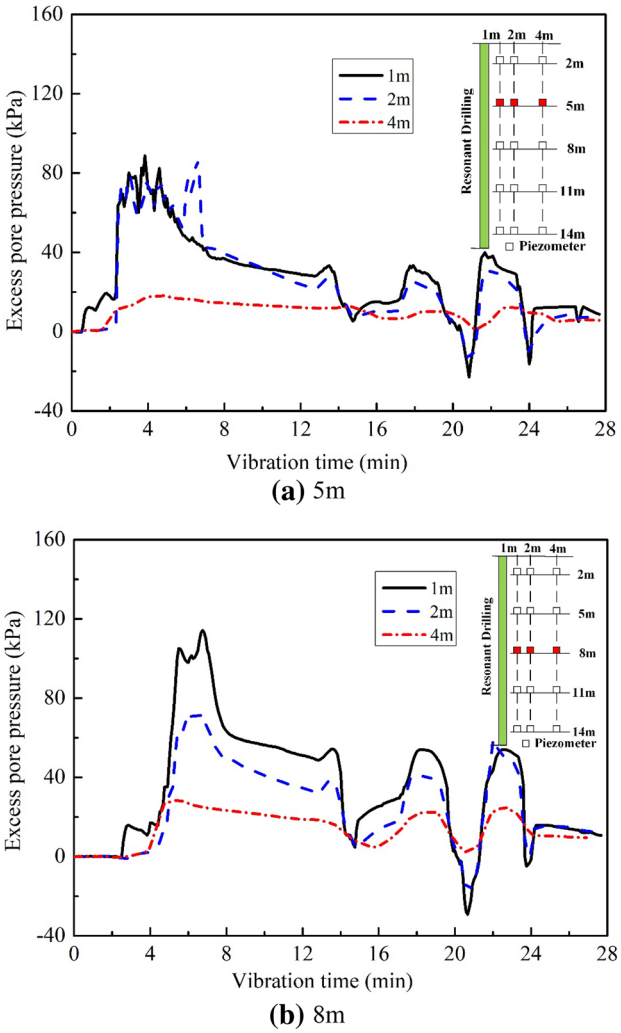

Fig. 11 Change of excess pore pressure at different distances from vibration point (K7+645): **a** 5 m; **b** 8 m

can be observed that the dissipation is almost over within 1 h of construction completion. The value of excess pore pressure at a distance of 1 m from the resonant drilling taking place 8 m below ground is larger and dissipates more slowly than other depths or locations due to the presence of a 10 cm-thin clay layer. More detailed and comprehensive analysis of dissipation curves of excess pore pressure measured by piezometers can be found in the literature [35]. In all, the pore pressure produced by the vibro-compaction dissipates very quickly and accelerates the speed of construction.

Figure 13 depicts the pore pressure dissipation process by CPTU at a depth of 5 and 8.1 m. The excess pore water pressure generated around the cone will start to dissipate when there is a pause in piezocone penetration. As shown in Fig. 14, when the resonant wing is inserted into the soil, the pore pressure is increasing from the initial pore pressure

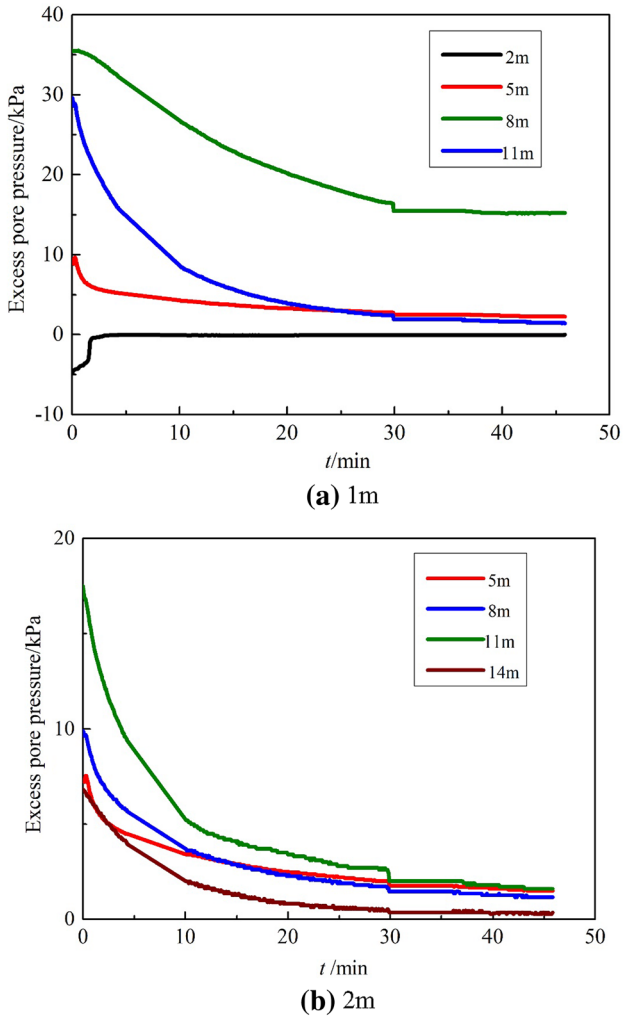

Fig. 12 Dissipation of excess pore pressure at 1 and 2 m from vibration point

−22.076, 38.888 kPa to the peak 52.808, 80.814 kPa (time required 840, 265 s), and then, the pore pressure is dissipating to 39.055, 65.146 kPa (total duration 2400, 1830s) for 5, 8.1 m, respectively. As time passes, the pore pressures measured by CPTU can eventually dissipate to hydrostatic pressures, which are consistent with the measured results of piezometers. This indicates that the CPTU testing can be applied to measure confined water.

6 Evaluation of the Effect of Reinforcement

The primary aim of the liquefiable ground is elimination of the liquefaction potential. An analytical approach for liquefaction potential evaluation is calculating a factor of safety (FS) that can be defined as follows:

$$\mathrm{FS} = \mathrm{CRR}/\mathrm{CSR}, \tag{8}$$

where CRR is the cyclic resistance ratio and CSR is the cyclic stress ratio induced by earthquake. The CSR values are always calculated using Seed's method [36], while CRR values can be estimated based on empirical correlations with in-situ testing parameters, particularly SPT testing and CPT/CPTU testing [37–40]. It is also known that the factor of safety (FS) can give more intuitive inspection of the liquefaction evaluation.

Figure 14 shows the FS estimation for two adjacent CPTU test bores and SPT drilling before and after vibro-compaction. FS values were less than 1.0 and with had high liquefaction potential before treatment. Moreover, a similar evaluation of liquefaction potential is achieved and confirmed for the SPT-based method [Code for Seismic Design of Buildings (GB50011-2010)] [41]. FS values greater than 1.0 after treatment indicate that the soil is densified, and elimination of the liquefaction potential is achieved. It can be concluded that vibro-compaction can result in elimination of the liquefaction potential and increase soil densification.

7 Discussion

Quality control and assurance of compaction often uses the penetration resistance index. It is known that the increase in penetration resistance is caused by a decrease in void ratio or an increase in stress. Thus, the index of void ratio or porosity can also be used to evaluate the effect of vibro-compaction. The porosity ratio of post-to-pre-densification can be obtained from the measured bulk resistivity ratio of pre-to-post-densification based on Archie's law. Therefore, the resistivity measurements may be a useful method to assess the densification of silty sand. The assumptions that the soil constants of Archie's law do not change during the process of vibro-compaction and that the soil is saturated, are needed, when using the method. In addition, how to evaluate the magnitude of soil volumetric strain from the resistivity measurements, particularly for RCPTU, requires further study.

An important, but often neglected, effect of vibro-compaction is high horizontal stress (i.e., ignoring K_o) caused by interaction friction between the probe surface and its surroundings [5]. The creation of strong horizontal stress pulses caused by the vertically oscillating probe will produce the permanent increases in horizontal stresses on the ground. This can be reflected by the change of K_o before and after treatment, as mentioned earlier. The creation of the preconsolidation effect caused by a constant increase in horizontal effective stress can be characterized by a rise in the overconsolidation ratio (OCR). Through the laboratory and CPTU test analyses, the OCR values have a significant increase, and are from uncompacted silty sand (OCR = 1) to more than

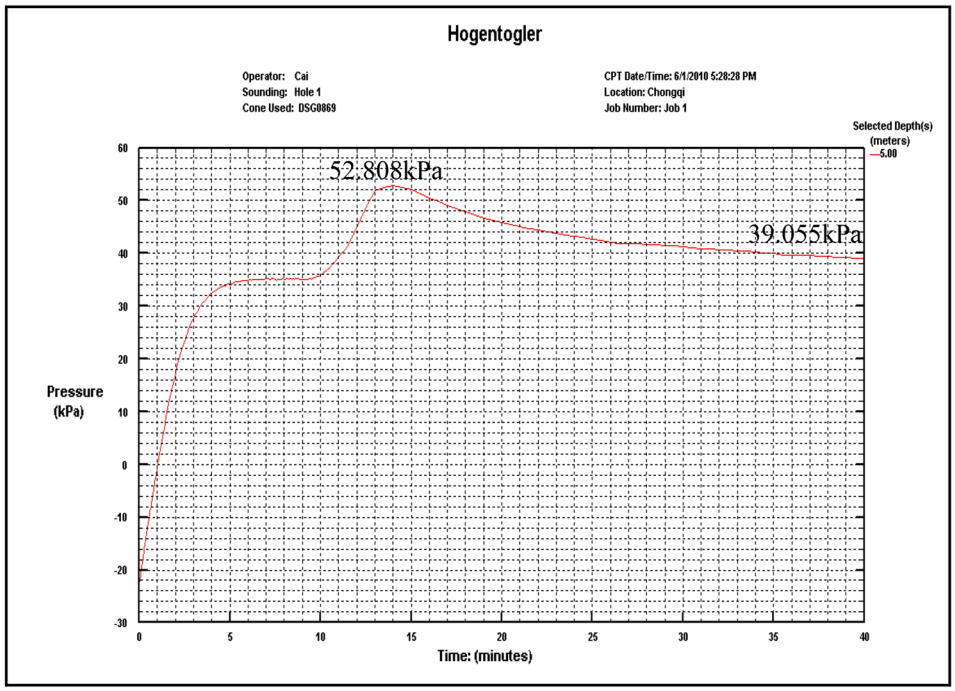

(a) 5m

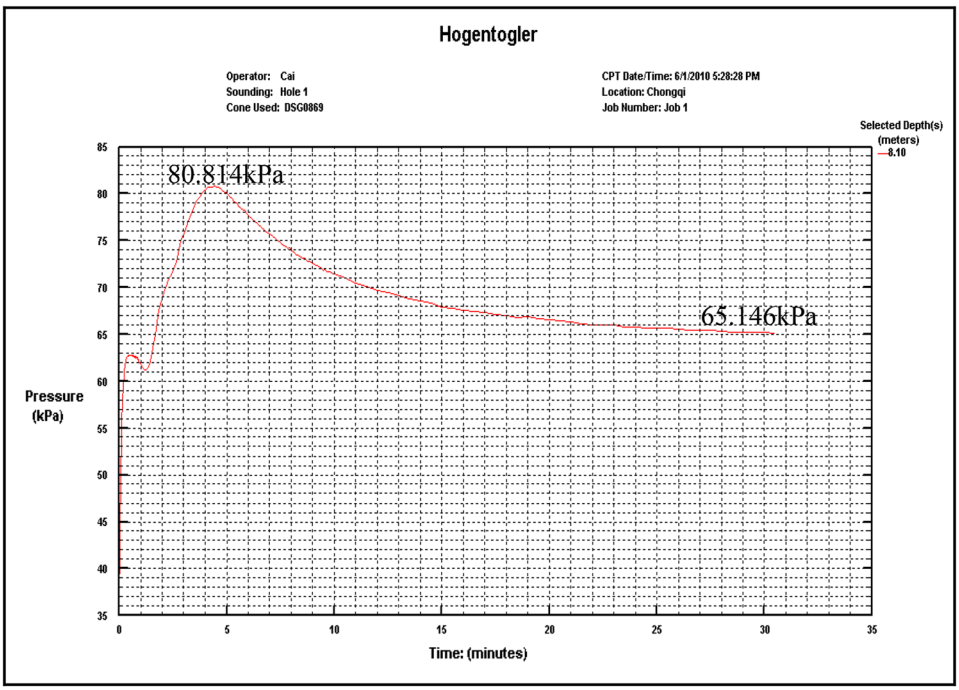

(b) 8.1m

Fig. 13 Dissipation of excess pore pressure from CPTU at two depths: **a** 5 m; **b** 8.10 m

1.0. It is indicated that there exists a preconsolidation effect, which can be reflected by the increase in sleeve friction.

Soil type can be evaluated using soil behavior type (SBT) charts. Figure 15 displays the records of some selected CPTU soundings plotted in the Robertson [42] soil classification charts prior to following vibro-compaction. It clearly shows the significant increase in sleeve friction and illustrates the increase in horizontal stress and OCR. This can be attributed to the often overlooked preconsolidation effect, which needs to be considered in the evaluation of compaction projects.

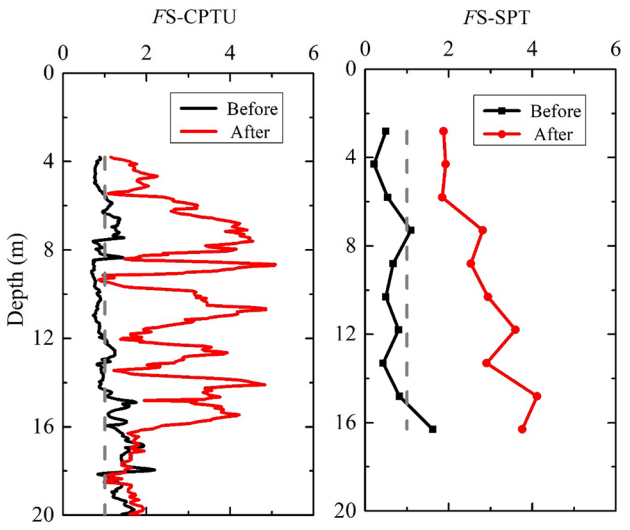

Fig. 14 Result of liquefaction evaluation before and after vibro-compaction

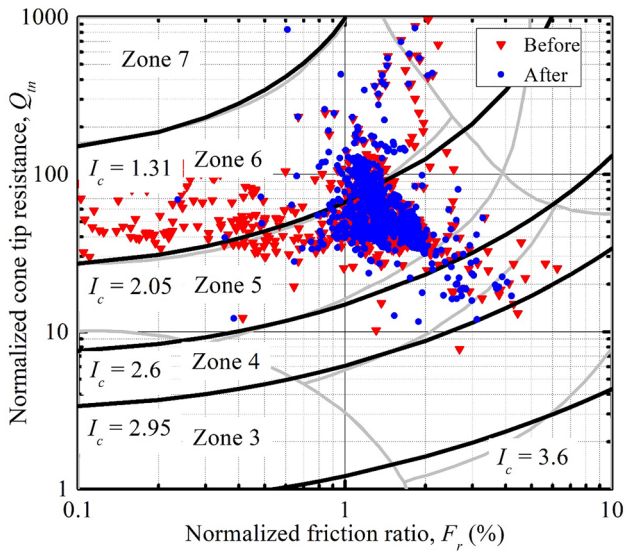

Fig. 15 Robertson [43] soil classification chart in study site

It was observed that excess pore pressures quickly dissipated after vibro-compaction (Figs. 13, 14), indicating that vibro-compaction can accelerate construction speed and improve the soil drainage system. Furthermore, the pore pressure reduction observed is in accord with the behavior of liquefied sand.

The settlement characteristics for vibro-compaction are always a key element of fine-grained soils. Based on the CPTU data, the estimate values of constrained modulus, E_s, increased from the 18.5 MPa to an average value of 38 MPa. The increase of the E_s is a highly desirable result which leads to a decrease in settlement.

8 Summary and Conclusions

A novel resonance compaction technique was used to improve ground liquefaction. This was achieved by evaluating the effectiveness of vibro-compaction on liquefied ground through penetration testing of RCPTU, SCPTU and SPT. The results reported indicate that a combination of penetration testing can give a comprehensive understanding of the changes in soil behavior prior to and following vibro-compaction. The following conclusions can be drawn:

1. The state parameter can represent the current state of the soil. The values of state parameter after treatment were further away from zero than the values prior to vibro-compaction. It was illustrated that soil state becomes denser as a result of vibro-compaction. V_s measurements were used to assess the small strain shear stiffness of the soil before and after vibro-compaction. The results indicated a clear increase in the soil strength and the degree of soil improvement.
2. The soil electrical resistivity measured during the piezo-cone penetration process can be applied to the evaluation of the densification effect of vibro-compaction. If it is assumed that the soil constants do not change in the process of compaction, the ratio of post-to-pre-densification porosity can be converted by the soil electrical resistivity based on Archie's law. The ratio of post-to-pre-densification porosity presented here is less than 1.0 due to compaction effect.
3. An important aspect of vibro-compaction of silty sand is the increased pf high horizontal stresses (i.e., ignoring K_o). The ratio of G_o from V_s measurements to tip resistance appears to provide information about changes in horizontal stress. The creation of a preconsolidation effect can be reflected by OCR or the increase of f_s. If it is assumed that uncompacted ground is normally consolidated (i.e., ignoring OCR = 1), the OCR has a significant increase after ground treatment. The Robertson [43]-modified soil classification charts can also provide further information on the increase in normalized friction or sleeve friction.
4. The liquefaction evaluation pre-and-post-vibro-compaction, in terms of FS, is made by the CPTU and SPT data. The results from CPTU and SPT are basically consistent and the FS values are more than 1.0 following treatment. The results indicate that vibro-compaction can eliminate liquefaction potential and can be used as an effective method to deal with liquefied ground.

Acknowledgements Majority of the work presented in this paper was funded by the National Key R&D Program of China (Grant No. 2016YFC0800200), the National Natural Science Foundation of China

(Grant No. 41672294), the Fundamental Research Funds for the Central Universities and Postgraduate Research & Practice Innovation Program of Jiangsu Province (KYCX17_0139). These financial supports are gratefully acknowledged. The authors also would like to thank Prof. Liyuan Tong, Guangyin Du, and YuanCheng for their assistance in field tests.

References

1. Massarsch KR, Fellenius BH (2002) Vibratory compaction of coarse-grained soils. Can Geotech J 39(3):695–709. https://doi.org/10.1139/t02-006
2. Bo MW, Arulrajah A, Horpibulsuk S, Leong M, Disfani MM (2013) Densification of land reclamation sands by deep vibratory compaction techniques. J Mater Civ Eng 26(8):06014016. https://doi.org/10.1061/(ASCE)MT.1943-5533.0001010
3. Cai G, Lin J, Liu S, Puppala AJ (2017) Characterization of spatial variability of CPTU data in a liquefaction site improved by vibro-compaction method. KSCE J Civ Eng 21(1):209–219. https://doi.org/10.1007/s12205-016-0631-1
4. Hussin JD (2006) Methods of soft ground improvement. The foundation engineering handbook. Taylor & Francis Group, New York, pp 529–565
5. Massarsch KR, Fellenius BH (2014) Use of CPT for design, monitoring, and performance verification of compaction projects. In: Proceedings Edited by Robertson, PK, Cabal, KL, pp 1187–1200
6. Tong B, Schaefer VR (2016) Optimization of vibrocompaction design for liquefaction mitigation of gravity caisson quay walls. Int J Geomech 16(4):04016005. https://doi.org/10.1061/(ASCE)GM.1943-5622.0000585
7. Juang CH, Ching J, Wang L, Khoshnevisan S, Ku CS (2013) Simplified procedure for estimation of liquefaction-induced settlement and site-specific probabilistic settlement exceedance curve using cone penetration test (CPT). Can Geotech J 50(10):1055–1066. https://doi.org/10.1139/cgj-2012-0410
8. Rollins KM, Kim J (2010) Dynamic compaction of collapsible soils based on US case histories. J Geotech Geoenviron Eng 136(9):1178–1186. https://doi.org/10.1061/(ASCE)GT.1943-5606.0000331
9. Zhou Y, Sun Z, Chen J, Chen Y, Chen R (2017) Shear wave velocity-based evaluation and design of stone column improved ground for liquefaction mitigation. Earthq Eng Eng Vibr 16(2):247–261. https://doi.org/10.1007/s11803-017-0380-2
10. Youd TL et al (2001) Liquefaction resistance of soils: summary report from the 1996 NCEER and 1998 NCEER/NSF workshops on evaluation of liquefaction resistance of soils [J]. J Geotech Geoenviron Eng 127(10):817–833. https://doi.org/10.1061/(ASCE)1090-0241(2001)127:10(817)
11. Cai G, Liu S, Puppala AJ (2012) Assessment of soft clay ground improvement from SCPTU results. Proc Inst Civ Eng Geotech Eng 165(2):83–95. https://doi.org/10.1680/geng.9.00081
12. Daniel CR, Howie JA, Campanella RG, Giacheti HL (1999) The resistivity piezocone penetration test (RCPTU) for quality control of geotechnical ground densification. In: Symposium on the application of geophysics to engineering and environmental problems (SAGEEP). Oakland, California, March, pp 133–142. https://doi.org/10.4133/1.2922599
13. Cheng Y, Liu S, Liu Z, Cai G (2012) Seismic cone penetration test assessment of vibratory probe compaction for liquefaction mitigation. In: GeoCongress 2012: state of the art and practice in geotechnical engineering, ASCE pp 1898–1907
14. Baziar MH, Ziaie-Moayed R (2006) Evaluation of cone penetration resistance in loose silty sand using calibration chamber. Int J Civ Eng 4(2):106–119
15. Campanella RG, Gillespie, Robertson PK (1982) Pore pressures during cone penetration testing. ESOPT-II, Proceedings of the second European symposium on penetration testing, Amsterdam. 2, A.A. Balkema, Rotterdam, pp 507–512
16. Baziar MH, Azizkandi AS, Kashkooli A (2015) Prediction of pile settlement based on cone penetration test results: an ANN approach. KSCE J Civ Eng 19(1):98–106. https://doi.org/10.1007/s12205-012-0628-3
17. Cai G, Chu Y, Liu S, Puppala AJ (2016) Evaluation of subsurface spatial variability in site characterization based on RCPTU data. Bull Eng Geol Env 75(1):401–412. https://doi.org/10.1007/s10064-015-0727-8
18. ASTM D5778 (2012) International standard test method for electronic friction cone and piezocone penetration testing of soils, annual book of ASTM standards. ASTM International, West Conshohocken
19. Lunne T, Robertson PK, Powell JJM (1997) Cone penetration testing in geotechnical practice. Blackie Academic and Professional, London
20. ISSMGE (1999) International reference test procedure (IRTP) for the cone penetration test (CPT) and the cone penetration test with pore pressure (CPTU). Report of the ISSMGE technical committee 16 on ground property characterization from in-situ testing. Proceedings of the 12th European conference of soil mechanics and geotechnical engineering, 3. Balkema, Amsterdam, pp 2195–2222
21. Dove JE, Boxill LEC, Jarrett JB (2000) A CPT-based index for evaluating ground improvement. Adv Grouting Ground Modif ASCE Geotech Spec Publ 104(GSP104):296–310
22. Massarsch KR, Fellenius BH (2017) Evaluation of resonance compaction of sand fills based on cone penetration tests. Proc Inst Civ Eng Ground Improv 170(3):149–158. https://doi.org/10.1680/jgrim.17.00004
23. Been K, Jefferies MG (1985) A state parameter for sands. Géotechnique 35(2):99–112. https://doi.org/10.1680/geot.1985.35.2.99
24. Jafarian Y, Abdollahi AS, Vakili R, Baziar MH (2010) Probabilistic correlation between laboratory and field liquefaction potentials using relative state parameter index (ξ_R). Soil Dyn Earthq Eng 30(10):1061–1072. https://doi.org/10.1016/j.soildyn.2010.04.017
25. Been K, Jefferies MG, Crooks JHA, Rothenburg L (1987) The cone penetration test in sands: part II, general inference of state. Geotechnique 37(3):285–299. https://doi.org/10.1680/geot.1987.37.3.285
26. Been K, Crooks JHA, Jefferies MG (1988) Interpretation of material state from the CPT in sands and clays. In: Penetration testing in the UK. Thomas Telford, London, pp 89–92
27. Jefferies MG, Been K (2006) Soil liquefaction—a critical state approach. Taylor and Francis Group, London **(ISBN 0-419-16170-8)**
28. Campanella RG, Martens S, Tomlinson S, Davies MP (1995) In-situ measurement of hydraulic conductivity in sands. In: Proceedings of 48th Canadian Geotechnical Conference, Canadian Geotechnical Society, Vancouver, BC, 1, pp 309–318
29. Howie JA, Daniel C, Asalemi AA, Campanella RG (2000) Combinations of in situ tests for control of ground modification in silts and sands. In Innovations and applications in geotechnical site characterization, pp 181–198
30. Zhang T, Cai G, Liu S, Duan W (2016) Laboratory observation of engineering properties and deformation mechanisms of cemented rubber–sand mixtures. Constr Build Mater 120:514–523. https://doi.org/10.1016/j.conbuildmat.2016.05.123
31. Mayne PW, Schneider JA, Martin GK (1999) Small-and large-strain soil properties from seismic fiat dilatometer tests. In: Jamiolkowski M, Lancellotta R, Lo Presti D (eds) Prefailure deformation of geomaterials: proceedings of the 2nd international

symposium, Torino, 1 ed. Taylor & Francis, Abingdon, pp 419–426
32. Hussien MN, Karray M (2015) Shear wave velocity as a geotechnical parameter: an overview. Can Geotech J 53(2):252–272. https://doi.org/10.1139/cgj-2014-0524
33. Baldi G, Bellotti R, Ghionna V, Jamiolkowski M, Pasqualini E (1986) Interpretation of CPTs and CPTUs-2nd part: drained penetration of sands. In Proceedings of 4th international geotechnical seminar on field instrumentation and in situ measurements, Nanyang Technology Institute, Singapore, pp 143–156
34. Eslaamizaad S, Robertson PK(1996) Estimation of in situ lateral stress and stress history in sands. In: Proceedings of 49th Canadian geotechnical conference S, Vol 1, pp 439–447
35. Liu S, Cheng Y (2012) Resonance compaction method for highway ground improvement at liquefaction site. China J Highway Transp 25(6):24–29 **(in Chinese)**
36. Seed HB, Idriss IM (1971) Simplified procedure for evaluating soil liquefaction potential. J Soil Mech Found Div ASCE 97(9):1249–1273
37. Cetin KO, Seed RB, Der Kiureghian A, Tokimatsu K, Harder JrLF, Kayen RE, Moss RE (2004) Standard penetration test-based probabilistic and deterministic assessment of seismic soil liquefaction potential. J Geotech Geoenviron Eng 130(12):1314–1340. https://doi.org/10.1061/(ASCE)1090-0241(2004)130:12(1314)
38. Yang Y, Chen L, Sun R, Chen Y, Wang W (2017) A depth-consistent SPT-based empirical equation for evaluating sand liquefaction. Eng Geol 221:41–49. https://doi.org/10.1016/j.enggeo.2017.02.032
39. Robertson PK, Wride CE (1998) Evaluating cyclic liquefaction potential using the cone penetration test. Can Geotech J 35(3):442–459. https://doi.org/10.1139/cgj-35-3-442
40. Boulanger RW, Idriss IM (2015) CPT-based liquefaction triggering procedure. J Geotech Geoenviron Eng 142(2):04015065. https://doi.org/10.1061/(ASCE)GT.1943-5606.0001388
41. Boncio P, Amoroso S, Vessia G, Francescone M, Nardone M, Monaco P, Galadini F (2018) Evaluation of liquefaction potential in an intermountain Quaternary lacustrine basin (Fucino basin, central Italy). Bull Earthq Eng 16(1):91–111. https://doi.org/10.1007/s10518-017-0201-z
42. Design Code (2010) Code for seismic design of buildings GB 50011-2010. China Architecture and Building Press, Beijing **(in Chinese)**
43. Robertson PK (2009) Interpretation of cone penetration tests—a unified approach. Can Geotech J 46(11):1337–1355. https://doi.org/10.1139/T09-065